https://doi.org/10.5607/en22027
Exp Neurobiol. 2022 Dec;31(6):409-418.
pISSN 1226-2560 • eISSN 2093-8144

Original Article

Experimental Neurobiology

XperCT-guided Intra-cisterna Magna Injection of Streptozotocin for Establishing an Alzheimer's Disease Model Using the Cynomolgus Monkey (*Macaca fascicularis*)

Junghyung Park[1†], Jinyoung Won[1†], Chang-Yeop Jeon[1], Kyung Seob Lim[2], Won Seok Choi[1], Sung-hyun Park[1], Jincheol Seo[1], Jiyeon Cho[1], Jung Bae Seong[1], Hyeon-Gu Yeo[1,3], Keonwoo Kim[1,4], Yu Gyeong Kim[1,3], Minji Kim[1,5], Kyung Sik Yi[6] and Youngjeon Lee[1,3*]

[1]National Primate Research Center, Korea Research Institute of Bioscience and Biotechnology (KRIBB), Cheongju 28116, [2]Futuristic Animal Resource and Research Center, Korea Research Institute of Bioscience and Biotechnology (KRIBB), Cheongju 28116, [3]KRIBB School of Bioscience, University of Science and Technology (UST), Daejeon 34113, [4]School of Life Sciences, BK21 Plus KNU Creative BioResearch Group, Kyungpook National University, Daegu 41566, [5]Department of Bio and Brain Engineering, Korea Advanced Institute of Science and Technology (KAIST), Daejeon 34141, [6]Department of Radiology, Chungbuk National University Hospital, Cheongju 28644, Korea

Till date, researchers have been developing animal models of Alzheimer's disease (AD) in various species to understand the pathological characterization and molecular mechanistic pathways associated with this condition in humans to identify potential therapeutic treatments. A widely recognized AD model that mimics the pathology of human AD involves the intracerebroventricular (ICV) injection with streptozotocin (STZ). However, ICV injection as an invasive approach has several limitations related to complicated surgical procedures. Therefore, in the present study, we created a customized stereotaxic frame using the XperCT-guided system for injecting STZ in cynomolgus monkeys, aiming to establish an AD model. The anatomical structures surrounding the cisterna magna (CM) were confirmed using CT/MRI fusion images of monkey brain with XperCT, the c-arm cone beam computed tomography. XperCT was used to determine the appropriate direction in which the needle tip should be inserted within the CM region. Cerebrospinal fluid (CSF) was collected to confirm the accurate target site when STZ was injected into the CM. Cynomolgus monkeys were administered STZ dissolved in artificial CSF once every week for 4 weeks via intracisterna magna (ICM) injection using XperCT-guided stereotactic system. The molecular mechanisms underlying the progression of STZ-induced AD pathology were analyzed two weeks after the final injection. The monkeys subjected to XperCT-based STZ injection via the ICM route showed features of AD pathology, including markedly enhanced neuronal loss, synaptic impairment, and tau phosphorylation in the hippocampus. These findings suggest a new approach for the construction of neurodegenerative disease models and development of therapeutic strategies.

Key words: Intra-cisterna magna, Streptozotocin, Alzheimer's disease, Cynomolgus monkey, Non-human primates

INTRODUCTION

The cisterna magna (CM) is the largest subarachnoid cistern between the arachnoid and pia mater layers; it receives cerebrospinal fluid (CSF) from the fourth ventricle [1]. The CSF continuously circulates in the cerebral ventricles, subarachnoid space, and spinal cord central canal while providing nourishment and protection to,

Submitted August 17, 2022, Revised November 14, 2022,
Accepted November 14, 2022

*To whom correspondence should be addressed.
TEL: 82-43-240-6316, FAX: 82-43-240-6309
e-mail: neurosci@kribb.re.kr
†These authors contributed equally to this article.

and enabling waste removal from, the brain [2]; CSF collection and intracisternal injection via suboccipital puncture are convenient strategies because they are less invasive and show a minimal risk of contamination [3]. Therefore, numerous studies using intracisternal administration of biologics, including adeno-associated virus (AAV)-mediated gene delivery and injection of antisense oligonucleotides (ASOs), recombinant enzymes, and novel agents as promising therapeutic candidates for neurodegenerative diseases, have demonstrated the medical efficacy of this technique and pathological mechanisms underlying various neurological diseases [4-6].

Intracisternal injection via suboccipital puncture with a manual stereotactic (non-stereotactic) and stereotactic method is widely used for drug distribution through CSF flow into the brain [7], since this method has several advantages. Although this route has diverse advantages for direct transport into the brain, the low accuracy of intracisternal injection remains a hurdle in the development of safe and reliable techniques for drug delivery. Intracisternal injection with a non-stereotactic method in particular requires anatomical knowledge and its efficacy depends on the skills and experience of the technician because otherwise, several side effects, including blood contamination, CSF leakage, and brain stem damage, can occur [8-10].

Alzheimer's disease (AD) is a progressive neurodegenerative disorder characterized by memory and cognitive decline [11]. Accumulation of amyloid-beta plaques and the formation of neurofibrillary tangles in the cerebral cortex and hippocampus are regarded as typical pathological hallmarks of AD [12, 13]. Furthermore, several abnormalities in brain glucose metabolism have been observed in AD patients. Cerebral impairment of insulin signaling and translation of insulin receptors have been recognized as early signs of AD progression [14-17].

Streptozotocin (STZ) is a diabetogenic compound generally used to establish animal models of diabetes owing to its ability to selectively impair the insulin signaling pathway [18]. Intracerebroventricular (ICV) administration of STZ disrupts the homeostasis of brain insulin signaling and defects in cerebral glucose metabolism [19]. This is accompanied by behavioral, neuropathological, and biochemical changes similar to those observed in the pathology of AD [20-22]. However, this technique is invasive and greatly limits the generalizability of the results obtained in monkeys. Although this technique is invasive method for studying the brain pathology in monkeys, there are some technical challenges and limitation to overcome unanticipated adverse effects. The ICM administration of STZ is also carried out, but much less frequently than ICV approach.

Therefore, the present study aimed to determine the effects of STZ administration in cynomolgus monkeys via the intra-cisterna magna (ICM) route using a novel technique for X-ray-based real-time three-dimensional imaging coupled with the c-arm cone beam computed tomography (CBCT) technology, XperCT (Philips), which can assess three-dimensional images of soft tissue, and bone structure; to the best of our knowledge, our study is the first to report the use of the XperCT stereotactic system for injecting drugs into the brain tissue to establish a monkey model of AD. We suggest a new alternative method for the stable and reproducible delivery of drugs or molecules in the brains of non-human primates (NHPs).

MATERIALS AND METHODS

Ethical statement

The experimental procedures using experimental animals were approved by the Institutional Animal Care and Use Committee of the Korea Research Institute of Bioscience and Biotechnology (KRIBB) Institutional Animal Care and Use Committee (Approval No. KRIBB-AEC-20253). The experimental procedures were performed in accordance with the national guidelines and in compliance with the Guide for the Care and Use of Laboratory Animals.

Experimental animals

Cynomolgus monkeys (*Macaca fascicularis*) were obtained from Suzhou Xishan Zhongke Laboratory Animal Co. (Suzhou, China); they were housed in individual indoor cages at the National Primate Research Center (NPRC) of the KRIBB, as described previously [23]. Cynomolgus monkeys were fed twice with commercially available monkey feed (Harlan, USA), supplemented with various fruits and water *ad libitum*. The health of the monkeys was monitored by the attending veterinarian, consistent with the recommendations of the Weatherall Report. Animal health monitoring for monkeys was performed via microbiological tests, including those for B virus, simian retrovirus (SRV), simian immunodeficiency virus (SIV), simian virus 40 (SV40), and simian T-cell lymphotropic virus (STLV), as described previously [24]. The animals were housed in a temperature-controlled room (24±2℃) with 50±5% humidity and a 12-h light/dark cycle.

Intra-cisterna magna (ICM) injection of STZ and CSF collection

The cisterna magna is located below the cerebellum, with an intact atlanto-occipital joint (Fig. 1). STZ (2 mg/kg; Sigma-Aldrich, St. Louis, MO, USA) was dissolved in artificial CSF (aCSF; Harvard Apparatus, Holliston, MA, USA). The custom-built ICM-stereotaxic frame used in the present study was designed for com-

https://doi.org/10.5607/en22027

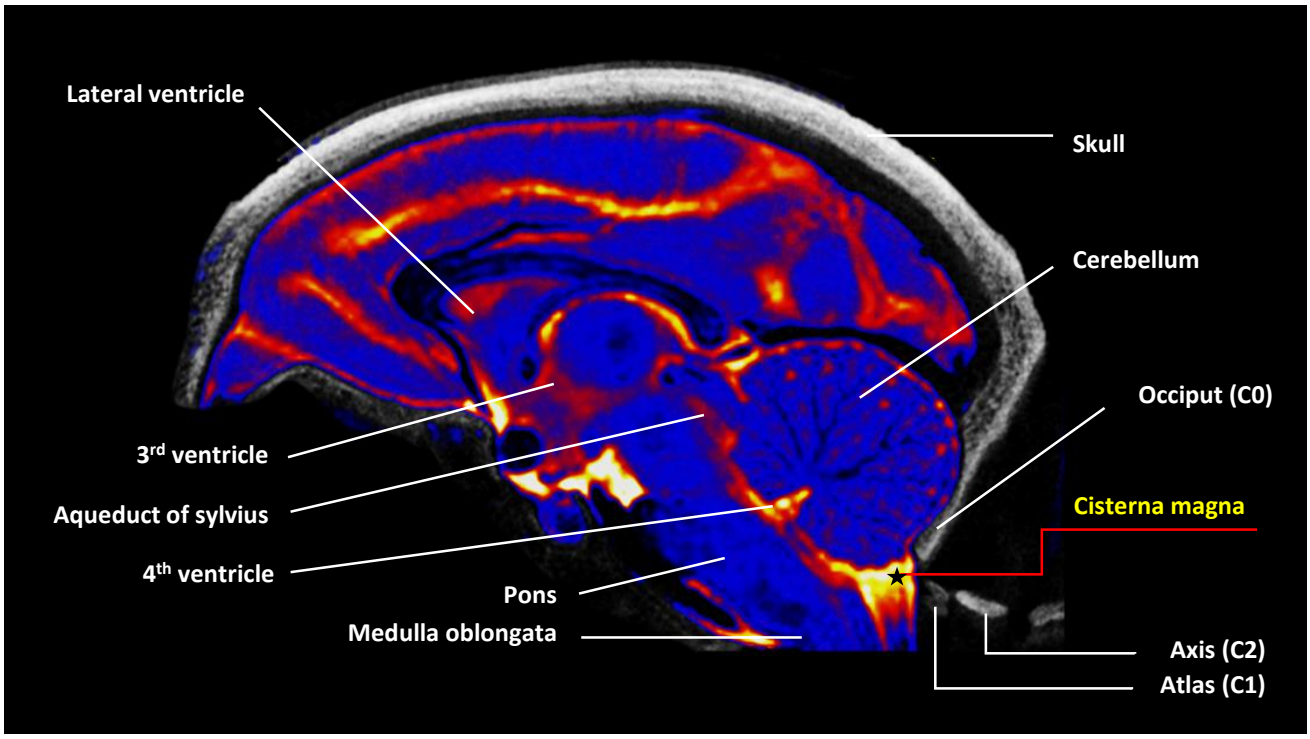

Fig. 1. Localization of the cisterna magna (CM) in monkey brain. The main anatomical structures surrounding cisterna magna in the monkey brain. Representative lateral CT/MRI fusion image showing the upper cervical spine joints, which comprised the occiput (C0), atlas (C1), and axis (C2).

patibility between CT and MRI (Fig. 2). All monkeys were initially anesthetized via the intraperitoneal injection of a cocktail mixture of ketamine (5 mg/kg) and atropine (0.02 mg/kg) and fixed in the sphinx position using a custom-built ICM-stereotaxic frame for image-guided stereotactic system under isoflurane-induced anesthesia (1.5% in 2 L/min oxygen). After confirmation of the correct needle tip position within the cisterna magna using XperCT imaging, CSF was extracted to verify the accurate position of the cisterna magna. Subsequently, the tube with the needle tip was connected to a Hamilton syringe containing STZ; ICM injections were administered once every week for 4 weeks.

MRI

MRI experiments were performed using a 3.0-T MRI scanner (Achieva 3.0T, Philips Medical Systems, Best, Netherlands) with an 8-channel knee coil. Three-dimensional (3D) sagittal T1-weighted images were acquired using the turbo field echo sequence with the following settings: TR/TE=14/6.8 ms, 128×128 field-of-view (FOV), matrix size 256×256, voxel size 0.5×0.5×0.5, and number of slices=150. The details of the MRI protocols were the same as those described in a previous report [25].

Blood and CSF analysis

Peripheral blood and CSF samples from all cynomolgus monkeys were collected, and cell type composition was analyzed using a hematology analyzer (Hemavet950; Drew Scientific, Miami Lakers, FL, USA).

Perfusion and tissue preparation

Two weeks after the final STZ injection, all cynomolgus monkeys were transcardially perfused with 500 ml of 100 mM phosphate-buffered solution (PBS) under deep anesthesia with the intramuscular injection of a cocktail of ketamine (5 mg/kg) and atropine (0.02 mg/kg). Whole brains were removed from the skull, washed with cold PBS, and separated bilaterally. Hippocampal proteins were harvested from monkey brains using punches on 4-mm-thick slices.

Western blot analysis

Protein samples of cynomolgus monkey hippocampi were harvested using the PRO-PREP protein extraction solution (Intron Biotechnology, Seongnam, Korea). Equal amounts (15 μg) of protein were separated by electrophoresis on 10~15% SDS-PAGE gels and transferred onto nitrocellulose membranes (BD Biosciences, Franklin Lakes, NJ, USA). The membranes were blocked by in-

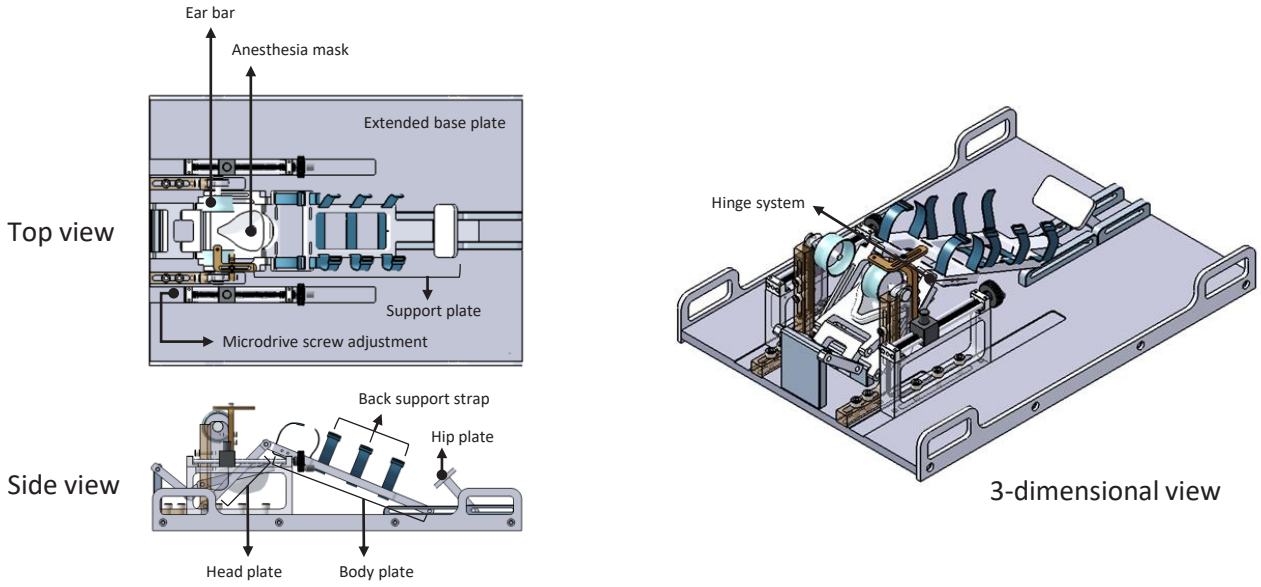

Fig. 2. Appearance of the custom-built CT-MRI compatible stereotaxic frame. The customized stereotaxic frame showing the top, side, and three-dimensional view. Top view shows the position of the extended base plate, the microdrive screw adjustment for the anteroposterior axis, anesthesia mask, ear bar, and support plate. Anteroposterior adjustment for adaptor is 150 mm. Side view shows the back strap and the support plates including head, body and hip for prone position. Three-dimensional view shows the hinge system, which are angle adjustable to stabilize and maintain the flexion of upper cervical spine.

cubation with blocking buffer (BD Biosciences) and probed with the following antibodies overnight at 4℃: anti-β-actin, anti-GFAP (Sigma-Aldrich, St. Louis, MO, USA), anti-NeuN, anti-synaptophysin, anti-PSD95, anti-phospho(p)-tau(S262), anti-p-tau(T181), and anti-p-tau(S396) (Abcam, MA, USA). Next, the membranes were washed with TBS saline containing 0.1% Tween-20 (TBST) and incubated with horseradish peroxidase-conjugated secondary antibodies (Cell Signaling, MA, USA) for 1 h at room temperature. After washing with TBST, the specific binding was detected using a chemiluminescence detection system (Thermo Scientific, MA, USA).

Statistical analysis

The data represent the mean±SD from three independent experiments (n≥3). Experimental differences were tested for statistical significance using two-way ANOVA conducted of variance using GraphPad Prism 9 software (San Diego, CA, USA). Statistical significance was set at $p<0.05$, and is indicated on the graphs using asterisks; p-values<0.01 and <0.001 were indicated by two and three asterisks, respectively.

RESULTS

T1-weighted MRI images obtained after the intracisternal tracer injection reveals the CSF dynamics

To develop a novel method for intracisternal injection using the XperCT-guided stereotactic system, we designed a protocol that enables the assessment of real-time updated images during the intervention. The animals were fixed in the sphinx position using a custom-built ICM-stereotaxic frame under anesthesia (Fig. 3A). After registration with the preoperative XperCT reconstruction, the planning and guiding needle insertion can be acquired to establish the path to the target site, i.e., the cisterna magna (CM). To verify the real-time position of the needle after insertion, we obtained a new XperCT image and confirmed the target point on the postoperative imaging (Fig. 3B). A CSF tracer was used to visualize the intracisternal injection through the target point. The CSF tracer (100 mM) was slowly injected (25 μl/min) into the CM, and brain T1-weighted MRI was performed after injection. Representative MRI images of tracer infusion into the CM showed the uptake of CSF into the brain parenchyma (Fig. 3C). These results suggest that the CSF tracer (injected via the ICM route) flows along the CSF circulation pathway and moves along the basement membrane of the brain parenchyma.

https://doi.org/10.5607/en22027

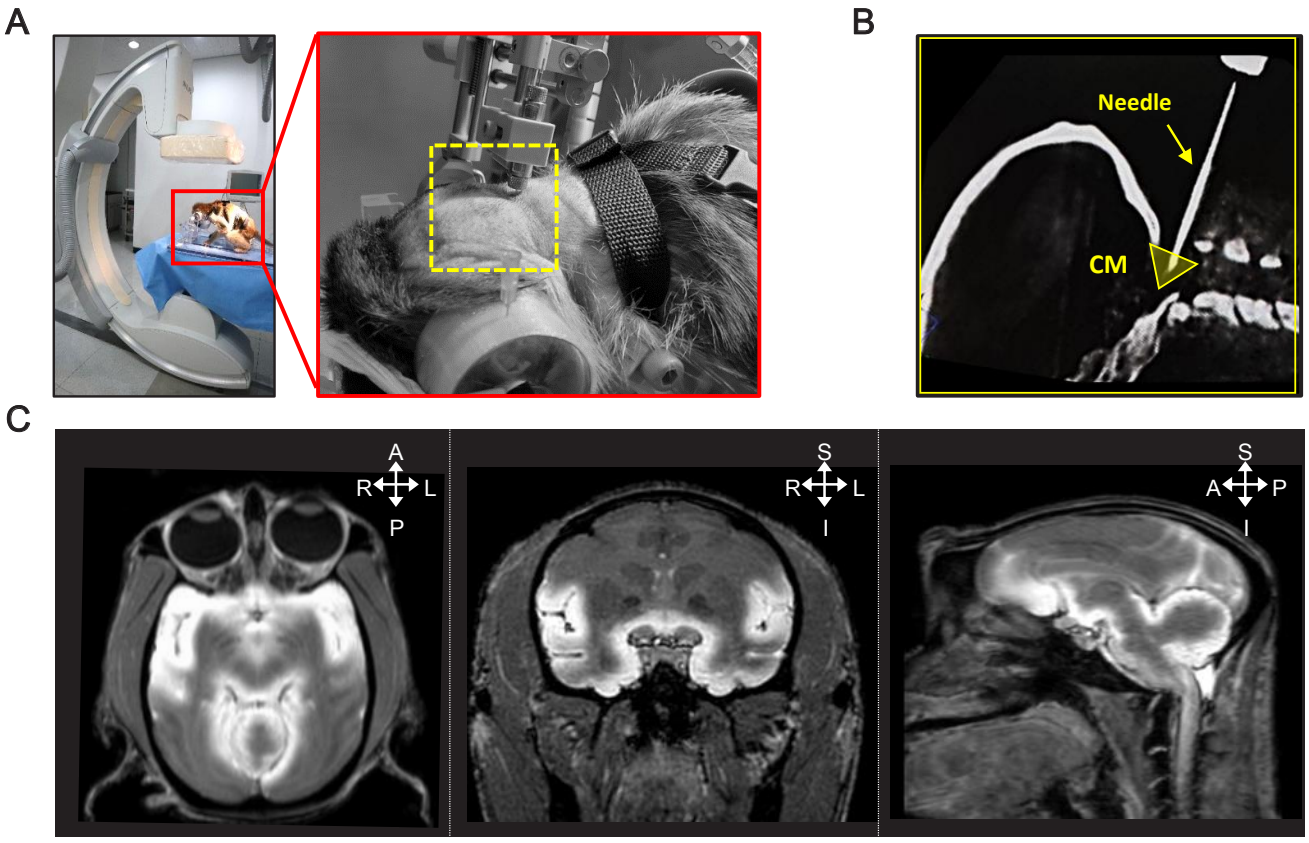

Fig. 3. Application of the custom-built CT-MRI compatible stereotaxic frame. (A) Picture of a monkey anesthetized and immobilized within a stereotaxic frame for XperCT scanning using the flat detector C-arm. (B) Representative XperCT image showing the accuracy and precision of the injection into the cisterna magna target region. (C) Representative MRI images obtained after the CSF tracer injection into the cisterna magna. The CSF tracer used is a gadolinium-based MR contrast agent.

Effects of STZ administration (via the ICM route) on AD pathology-associated features in hippocampus of cynomolgus monkeys

To apply the XperCT-guided ICM administration system, we selected STZ, which is known to trigger AD pathology in cynomolgus monkeys [25-27]. We injected aCSF (vehicle group; *n*=2) and STZ (2 mg/kg; STZ group; *n*=2) using XperCT-guided ICM at weeks 1, 2, 3, and 4 (Table 1). Two weeks after the last ICM-STZ administration, all monkeys were sacrificed and further protein analysis was performed (Table 2 and Fig. 4A). Given that several studies have suggested that STZ successfully triggers AD pathology-associated features, such as neuronal loss, synaptic loss, and abnormal tau phosphorylation [28-31], we analyzed neuronal loss, synaptic loss, and abnormal tau phosphorylation by immunoblotting analysis. STZ-induced neuronal loss was confirmed by assessing the levels of the NeuN protein, a neuronal marker. The NeuN protein levels decreased significantly in the STZ-injected group (Fig. 4B). In addition, we determined the expression levels of the pre- and post-synaptic proteins synaptophysin and PSD95, respectively. The expression levels of synaptophysin and PSD95 in the hippocampus decreased in the mice from the STZ-injected group (Fig. 4C). We also verified that the phosphorylation the of tau epitopes, i.e., the levels of p-Tau(S262), increased significantly in the mice from the STZ-injected groups (Fig. 4D), whereas the levels of p-Tau(T181) and p-Tau(S396) seemed to be more affected by individual differences (Fig. 4E). These results indicate that diverse AD pathology-associated features were observed in the hippocampus of cynomolgus monkeys injected with STZ via the ICM route.

DISCUSSION

The ICM route of administration has been continuously developed for enhanced central nervous system (CNS) drug delivery. This method is widely used to bypass the blood-brain barrier and has distinct advantages for direct delivery into the CNS [32]. An alternative to CSF-mediated delivery routes is lumbar intrathecal (IT) injection and ICV infusion. However, IT injection via lumbar puncture and ICV infusion via cranial puncture are challenging

Table 1. Differential count of Leukocytes and Erythrocytes in blood and CSF from cynomolgus monkeys

	Leukocytes					Erythrocytes	
	WBC (10^3/μl)	Neutrophils (10^3/μl)	Lymphocytes (10^3/μl)	Monocytes (10^3/μl)	Eosinophils (10^3/μl)	RBC (10^3/μl)	Hb (g/dl)
Blood	9.9±4.0	6.6±3.9	2.7±1.7	0.2±0.1	0.3±0.2	5.5±0.6	11.5±1.3
CSF	0.0±0.0	0.0±0.0	0.0±0.0	0.0±0.0	0.0±0.0	0.0±0.0	0.0±0.0

WBC, white blood cell; RBC, red blood cell; Hb, hemoglobin; CSF, cerebrospinal fluid.

Table 2. Summary of NHPs in this study

Group	Label	Gender	Age (years)	Weight (kg)	Dose (mg/kg)
Vehicle	C1	Female	6	2.9	-
	C2	Female	7	2.9	
STZ	C3	Female	10	3.2	2
	C4	Female	8	2.8	

because of procedural complexity, risk of possible contamination, and postoperative complications [33-35]. Lumbar puncture used to obtain CSF or for chemotherapy is a highly skilled procedure that requires practical experience and specific knowledge of the relevant anatomy. In addition, cranial puncture site infections and intracerebral hemorrhage after ICV infusion are inherent surgical risks. Therefore, ICM administration has a clear advantage, given that it is widely used in animal models. In addition, the ICM route has been used extensively, particularly in NHPs, because it offers the easiest entry into the ventricles of the brain and subarachnoid space around the brain and spinal cord, except for craniotomy [36].

Although there are infectious and non-infectious complications related to ICM injection, they can be controlled and prevented by improving the accuracy of ICM injection using advanced radiologic techniques such as X-ray, CT, and MRI [3, 37, 38]. Here, we describe the design of an XperCT-guided stereotactic system to optimize high-precision and stable CSF collection without multiple complications. To achieve X-ray-based real-time 3D imaging during the ICM targeting procedure, we used a newly developed system, the XperCT technology. The XperCT-guided technique allows precise planning of access to ensure injection of the drug at an appropriate position to avoid brainstem injury [39]. Therefore, the XperCT-guided ICM injection technique described herein provides evidence to support the wide applicability of the stereotaxic procedure of NHPs.

NHPs, including cynomolgus monkeys (*Macaca fascicularis*), share brain structure and function and are genetically similar to humans [40]. Moreover, AD-related natural processes in the brains of some aged NHPs are similar to those in humans [41-43]. Therefore, there is a need for an NHP-based model that reflects the AD pathology-associated features observed in humans. To date, several groups have developed transgenic monkey models expressing human mutant transgenes characteristic of the familial form of AD, such as the amyloid-β precursor protein or Tau protein [44, 45]. Although these transgenic models are valuable tools for studying the molecular mechanisms underlying AD pathogenesis, they do not fully replicate certain aspects of the neuropathology of AD. Therefore, non-transgenic AD models have become an important focus of research. Administration of STZ via the ICV route causes the establishment of an insulin-resistant brain state, a prominent representative feature of non-transgenic AD models; this feature has been proposed as a well-characterized, and is considered an appropriate, AD pathology-associated feature [19-22, 29]. However, a major disadvantage of ICV injection is that it is an invasive procedure involving a skin incision and trauma to the brain tissue. Earlier studies have confirmed that accurate and reproducible access to the CSF using ICM injection ensures the diffusion of the drug into the parenchyma and is similar to the diffusion observed after ICV injection [46, 47]. Therefore, we previously developed a clinically relevant STZ-administered AD model using ICM injection in monkeys and rats, which is characterized by cerebral damage, disintegration of the neurovascular unit, neuroinflammation, amyloid deposition, neuronal loss, and tau phosphorylation [25, 27, 48]. However, there are some technical challenges and limitations to constructing stable and reproducible AD NHP-based models, including high costs and skilled technical infrastructure of XperCT. To the best of our knowledge, the present study is the first to apply the XperCT-guided system to achieve the stable and reproducible establishment of NHP models of AD via intracisternal STZ administration using a custom-built ICM-stereotaxic frame. Pathological and molecular changes, such as neuronal loss, synaptic impairment, and hyperphosphorylation of Tau, were observed in our NHP model of STZ-induced AD. However, other typical AD hallmarks, such as astrocyte and microglial activation, between the animals in the vehicle and STZ groups were not significantly different. To overcome the limitations of our results, such as low sample size, additional experimental conditions, such as the examination of more than two monkeys per group and/

https://doi.org/10.5607/en22027

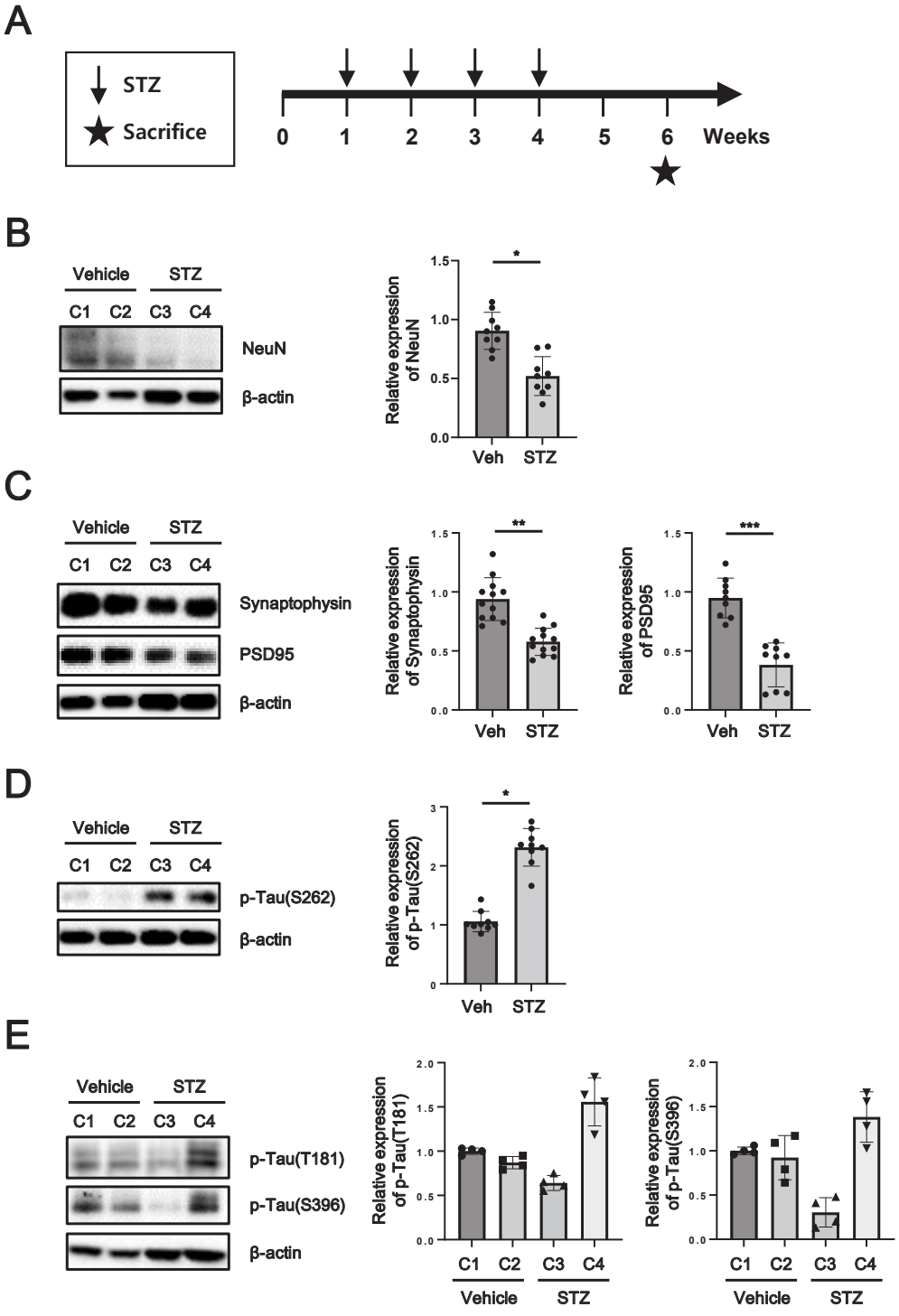

Fig. 4. STZ (injected via the ICM route)-induced AD pathology in the hippocampus of cynomolgus monkeys. (A) A schematic diagram of the experimental schedule. The expression levels of (B) NeuN, (C) Synaptophysin and PSD95, (D) p-Tau(S262), and (E) p-Tau(T181) and p-Tau(S396) with equal amount protein sample (15 μg) of hippocampus in vehicle- or STZ-injected cynomolgus monkeys were determined using western blotting analysis. * denotes $p<0.05$, ** denotes $p<0.01$, and *** denotes $p<0.001$.

or at various time points, are required. Moreover, in the monkey model of AD described in the present study, MRI scans (showing prominent ventricular dilation and parenchymal atrophy) and evaluation of cognitive function were not performed. Therefore, we believe that diverse observations, such as long-term follow-up observation of changes in cognitive function [49], brain scans us-

ing MRI [50], and AD marker screening from CSF and blood [51] are required to obtain more accurate information regarding STZ-induced AD monkey models.

Taken together, we designed and applied a new alternative method, i.e., the XperCT-guided injection method, as a stable and reproducible delivery system for administering drugs into the brains of NHPs via the ICM route. Our findings suggest that this new approach can be applied for the delivery of diverse molecules, such as drugs, ASOs, viral vectors, and disease inducers, into brain tissues.

ACKNOWLEDGEMENTS

This study was supported by the Korea Research Institute of Bioscience and Biotechnology Research Initiative Program (KGM4562222 and KGM5282221), and by the National Research Council of Science & Technology (NST) grant by the Korea government (MSIT) (No. CPS21101-100), and by the Korea Medical Device Development Fund grant funded by the Korea government (the Ministry of Science and ICT, the Ministry of Trade, Industry and Energy, the Ministry of Health & Welfare, the Ministry of Food and Drug Safety) (Project Number: 9991006929, RS-2020-KD000264).

REFERENCES

1. Ward E, Orrison WW, Watridge CB (1989) Anatomic evaluation of cisternal puncture. Neurosurgery 25:412-415.
2. Lehtinen MK, Bjornsson CS, Dymecki SM, Gilbertson RJ, Holtzman DM, Monuki ES (2013) The choroid plexus and cerebrospinal fluid: emerging roles in development, disease, and therapy. J Neurosci 33:17553-17559.
3. Li X, Han P, Guo Y, Sun H, Xiao Y, Kang YJ (2015) An improved technique for cerebrospinal fluid collection of cisterna magna in Rhesus monkeys. J Neurosci Methods 249:59-65.
4. Liguore WA, Domire JS, Button D, Wang Y, Dufour BD, Srinivasan S, McBride JL (2019) AAV-PHP.B administration results in a differential pattern of CNS biodistribution in non-human primates compared with mice. Mol Ther 27:2018-2037.
5. Hull V, Wang Y, Burns T, Zhang S, Sternbach S, McDonough J, Guo F, Pleasure D (2020) Antisense oligonucleotide reverses leukodystrophy in Canavan disease mice. Ann Neurol 87:480-485.
6. Mader KM, Beard H, King BM, Hopwood JJ (2008) Effect of high dose, repeated intra-cerebrospinal fluid injection of sulphamidase on neuropathology in mucopolysaccharidosis type IIIA mice. Genes Brain Behav 7:740-753.
7. Perez BA, Shutterly A, Chan YK, Byrne BJ, Corti M (2020) Management of neuroinflammatory responses to AAV-mediated gene therapies for neurodegenerative diseases. Brain Sci 10:119.
8. Gilberto DB, Zeoli AH, Szczerba PJ, Gehret JR, Holahan MA, Sitko GR, Johnson CA, Cook JJ, Motzel SL (2003) An alternative method of chronic cerebrospinal fluid collection via the cisterna magna in conscious rhesus monkeys. Contemp Top Lab Anim Sci 42:53-59.
9. Barthel L, Engler H, Hadamitzky M, Lückemann L, Sure U, Schedlowski M, Hetze S (2021) A step-by-step guide for microsurgical collection of uncontaminated cerebrospinal fluid from rat cisterna magna. J Neurosci Methods 352:109085.
10. Romagnoli N, Ventrella D, Giunti M, Dondi F, Sorrentino NC, Fraldi A, Surace EM, Bacci ML (2014) Access to cerebrospinal fluid in piglets via the cisterna magna: optimization and description of the technique. Lab Anim 48:345-348.
11. Hardy J (2006) A hundred years of Alzheimer's disease research. Neuron 52:3-13.
12. Querfurth HW, LaFerla FM (2010) Alzheimer's disease. N Engl J Med 362:329-344.
13. Kesslak JP, Nalcioglu O, Cotman CW (1991) Quantification of magnetic resonance scans for hippocampal and parahippocampal atrophy in Alzheimer's disease. Neurology 41:51-54.
14. Moloney AM, Griffin RJ, Timmons S, O'Connor R, Ravid R, O'Neill C (2010) Defects in IGF-1 receptor, insulin receptor and IRS-1/2 in Alzheimer's disease indicate possible resistance to IGF-1 and insulin signalling. Neurobiol Aging 31:224-243.
15. Liu Y, Liu F, Grundke-Iqbal I, Iqbal K, Gong CX (2011) Deficient brain insulin signalling pathway in Alzheimer's disease and diabetes. J Pathol 225:54-62.
16. Talbot K, Wang HY, Kazi H, Han LY, Bakshi KP, Stucky A, Fuino RL, Kawaguchi KR, Samoyedny AJ, Wilson RS, Arvanitakis Z, Schneider JA, Wolf BA, Bennett DA, Trojanowski JQ, Arnold SE (2012) Demonstrated brain insulin resistance in Alzheimer's disease patients is associated with IGF-1 resistance, IRS-1 dysregulation, and cognitive decline. J Clin Invest 122:1316-1338.
17. Bomfim TR, Forny-Germano L, Sathler LB, Brito-Moreira J, Houzel JC, Decker H, Silverman MA, Kazi H, Melo HM, McClean PL, Holscher C, Arnold SE, Talbot K, Klein WL, Munoz DP, Ferreira ST, De Felice FG (2012) An anti-diabetes agent protects the mouse brain from defective insulin signaling caused by Alzheimer's disease- associated Aβ oligomers. J

Clin Invest 122:1339-1353.
18. Lee W, Wakasugi H, Ibayashi H (1983) Comparison of somatostatin distribution in pancreatic duct ligated rats and streptozotocin diabetic rats. Gastroenterol Jpn 18:453-458.
19. Grieb P (2016) Intracerebroventricular streptozotocin injections as a model of Alzheimer's disease: in search of a relevant mechanism. Mol Neurobiol 53:1741-1752.
20. Salkovic-Petrisic M, Hoyer S (2007) Central insulin resistance as a trigger for sporadic Alzheimer-like pathology: an experimental approach. J Neural Transm Suppl 72:217-233.
21. Correia SC, Santos RX, Perry G, Zhu X, Moreira PI, Smith MA (2011) Insulin-resistant brain state: the culprit in sporadic Alzheimer's disease? Ageing Res Rev 10:264-273.
22. Kamat PK (2015) Streptozotocin induced Alzheimer's disease like changes and the underlying neural degeneration and regeneration mechanism. Neural Regen Res 10:1050-1052.
23. Yeo HG, Hong JJ, Lee Y, Yi KS, Jeon CY, Park J, Won J, Seo J, Ahn YJ, Kim K, Baek SH, Hwang EH, Kim G, Jin YB, Jeong KJ, Koo BS, Kang P, Lim KS, Kim SU, Huh JW, Kim YH, Son Y, Kim JS, Choi CH, Cha SH, Lee SR (2019) Increased CD68/TGFβ co-expressing microglia/ macrophages after transient middle cerebral artery occlusion in rhesus monkeys. Exp Neurobiol 28:458-473.
24. Jeong HS, Lee SR, Kim JE, Lyoo IK, Yoon S, Namgung E, Chang KT, Kim BS, Yang S, Im JJ, Jeon S, Kang I, Ma J, Chung YA, Lim SM (2018) Brain structural changes in cynomolgus monkeys administered with 1-methyl-4-phenyl-1,2,3,6-tetrahydropyridine: a longitudinal voxel-based morphometry and diffusion tensor imaging study. PLoS One 13:e0189804.
25. Yeo HG, Lee Y, Jeon CY, Jeong KJ, Jin YB, Kang P, Kim SU, Kim JS, Huh JW, Kim YH, Sim BW, Song BS, Park YH, Hong Y, Lee SR, Chang KT (2015) Characterization of cerebral damage in a monkey model of Alzheimer's disease induced by intracerebroventricular injection of streptozotocin. J Alzheimers Dis 46:989-1005.
26. Park SJ, Kim YH, Lee Y, Kim KM, Kim HS, Lee SR, Kim SU, Kim SH, Kim JS, Jeong KJ, Lee KM, Huh JW, Chang KT (2013) Selection of appropriate reference genes for RT-qPCR analysis in a streptozotocin-induced Alzheimer's disease model of cynomolgus monkeys (*Macaca fascicularis*). PLoS One 8:e56034.
27. Park SJ, Kim YH, Nam GH, Choe SH, Lee SR, Kim SU, Kim JS, Sim BW, Song BS, Jeong KJ, Lee Y, Park YI, Lee KM, Huh JW, Chang KT (2015) Quantitative expression analysis of APP pathway and tau phosphorylation-related genes in the ICV STZ-induced non-human primate model of sporadic Alzheimer's disease. Int J Mol Sci 16:2386-2402.
28. Planel E, Tatebayashi Y, Miyasaka T, Liu L, Wang L, Herman M, Yu WH, Luchsinger JA, Wadzinski B, Duff KE, Takashima A (2007) Insulin dysfunction induces in vivo tau hyperphosphorylation through distinct mechanisms. J Neurosci 27:13635-13648.
29. Chen Y, Liang Z, Blanchard J, Dai CL, Sun S, Lee MH, Grundke-Iqbal I, Iqbal K, Liu F, Gong CX (2013) A non-transgenic mouse model (icv-STZ mouse) of Alzheimer's disease: similarities to and differences from the transgenic model (3xTg-AD mouse). Mol Neurobiol 47:711-725.
30. Omidi G, Karimi SA, Shahidi S, Faraji N, Komaki A (2020) Coenzyme Q10 supplementation reverses diabetes-related impairments in long-term potentiation induction in hippocampal dentate gyrus granular cells: an in vivo study. Brain Res 1726:146475.
31. Kamat PK, Kalani A, Rai S, Tota SK, Kumar A, Ahmad AS (2016) Streptozotocin intracerebroventricular-induced neurotoxicity and brain insulin resistance: a therapeutic intervention for treatment of sporadic Alzheimer's disease (sAD)-like pathology. Mol Neurobiol 53:4548-4562.
32. Gray SJ, Woodard KT, Samulski RJ (2010) Viral vectors and delivery strategies for CNS gene therapy. Ther Deliv 1:517-534.
33. Kuo A, Smith MT (2014) Theoretical and practical applications of the intracerebroventricular route for CSF sampling and drug administration in CNS drug discovery research: a mini review. J Neurosci Methods 233:166-171.
34. Cohen-Pfeffer JL, Gururangan S, Lester T, Lim DA, Shaywitz AJ, Westphal M, Slavc I (2017) Intracerebroventricular delivery as a safe, long-term route of drug administration. Pediatr Neurol 67:23-35.
35. Wang Y, Qiu L, Dong J, Wang B, Shi Z, Liu B, Wang W, Zhang J, Cai S, Ye G, Cai X (2013) Comparison of the pharmacokinetics of imipenem after intravenous and intrathecal administration in rabbits. Eur Rev Med Pharmacol Sci 17:711-719.
36. Kondratov O, Kondratova L, Mandel RJ, Coleman K, Savage MA, Gray-Edwards HL, Ness TJ, Rodriguez-Lebron E, Bell RD, Rabinowitz J, Gamlin PD, Zolotukhin S (2021) A comprehensive study of a 29-capsid AAV library in a non-human primate central nervous system. Mol Ther 29:2806-2820.
37. Katz N, Goode T, Hinderer C, Hordeaux J, Wilson JM (2018) Standardized method for intra-cisterna magna delivery under fluoroscopic guidance in nonhuman primates. Hum Gene Ther Methods 29:212-219.
38. Hinderer C, Bell P, Vite CH, Louboutin JP, Grant R, Bote E, Yu H, Pukenas B, Hurst R, Wilson JM (2014) Widespread gene transfer in the central nervous system of cynomolgus ma-

caques following delivery of AAV9 into the cisterna magna. Mol Ther Methods Clin Dev 1:14051.
39. Racadio JM, Babic D, Homan R, Rampton JW, Patel MN, Racadio JM, Johnson ND (2007) Live 3D guidance in the interventional radiology suite. AJR Am J Roentgenol 189:W357-W364.
40. Podlisny MB, Tolan DR, Selkoe DJ (1991) Homology of the amyloid beta protein precursor in monkey and human supports a primate model for beta amyloidosis in Alzheimer's disease. Am J Pathol 138:1423-1435.
41. Chen JA, Fears SC, Jasinska AJ, Huang A, Al-Sharif NB, Scheibel KE, Dyer TD, Fagan AM, Blangero J, Woods R, Jorgensen MJ, Kaplan JR, Freimer NB, Coppola G (2018) Neurodegenerative disease biomarkers $A\beta_{1-40}$, $A\beta_{1-42}$, tau, and p-tau_{181} in the vervet monkey cerebrospinal fluid: relation to normal aging, genetic influences, and cerebral amyloid angiopathy. Brain Behav 8:e00903.
42. Zhang J, Chen B, Lu J, Wu Y, Wang S, Yao Z, Zhu L, Qiao Y, Sun Q, Qin W, Zhao Q, Jia J, Wei C (2019) Brains of rhesus monkeys display Aβ deposits and glial pathology while lacking Aβ dimers and other Alzheimer's pathologies. Aging Cell 18:e12978.
43. Cramer PE, Gentzel RC, Tanis KQ, Vardigan J, Wang Y, Connolly B, Manfre P, Lodge K, Renger JJ, Zerbinatti C, Uslaner JM (2018) Aging African green monkeys manifest transcriptional, pathological, and cognitive hallmarks of human Alzheimer's disease. Neurobiol Aging 64:92-106.
44. Beckman D, Chakrabarty P, Ott S, Dao A, Zhou E, Janssen WG, Donis-Cox K, Muller S, Kordower JH, Morrison JH (2021) A novel tau-based rhesus monkey model of Alzheimer's pathogenesis. Alzheimers Dement 17:933-945.
45. Seita Y, Morimura T, Watanabe N, Iwatani C, Tsuchiya H, Nakamura S, Suzuki T, Yanagisawa D, Tsukiyama T, Nakaya M, Okamura E, Muto M, Ema M, Nishimura M, Tooyama I (2020) Generation of transgenic cynomolgus monkeys overexpressing the gene for amyloid-β precursor protein. J Alzheimers Dis 75:45-60.
46. Chen Y, Imai H, Ito A, Saito N (2013) Novel modified method for injection into the cerebrospinal fluid via the cerebellomedullary cistern in mice. Acta Neurobiol Exp (Wars) 73:304-311.
47. Proescholdt MG, Hutto B, Brady LS, Herkenham M (2000) Studies of cerebrospinal fluid flow and penetration into brain following lateral ventricle and cisterna magna injections of the tracer [14C]inulin in rat. Neuroscience 95:577-592.
48. Ahn Y, Seo J, Park J, Won J, Yeo HG, Kim K, Jeon CY, Huh JW, Lee SR, Lee DS, Lee Y (2020) Synaptic loss and amyloid beta alterations in the rodent hippocampus induced by streptozotocin injection into the cisterna magna. Lab Anim Res 36:17.
49. Kim K, Jeon HA, Seo J, Park J, Won J, Yeo HG, Jeon CY, Huh JW, Kim YH, Hong Y, Choi JW, Lee Y (2020) Evaluation of cognitive function in adult rhesus monkeys using the finger maze test. Appl Anim Behav Sci 224:104945.
50. Heuer E, Jacobs J, Du R, Wang S, Keifer OP, Cintron AF, Dooyema J, Meng Y, Zhang X, Walker LC (2017) Amyloid-related imaging abnormalities in an aged squirrel monkey with cerebral amyloid angiopathy. J Alzheimers Dis 57:519-530.
51. Beckman D, Ott S, Donis-Cox K, Janssen WG, Bliss-Moreau E, Rudebeck PH, Baxter MG, Morrison JH (2019) Oligomeric Aβ in the monkey brain impacts synaptic integrity and induces accelerated cortical aging. Proc Natl Acad Sci U S A 116:26239-26246.